MOLECULAR AND CELLULAR BIOLOGY, Aug. 2008, p. 5106–5119 Vol. 28, No. 16
0270-7306/08/$08.00+0 doi:10.1128/MCB.00060-08
Copyright © 2008, American Society for Microbiology. All Rights Reserved.

# Reactive Oxygen Species Regulate Hypoxia-Inducible Factor 1α Differentially in Cancer and Ischemia▽†

Amina A. Qutub* and Aleksander S. Popel

*Department of Biomedical Engineering, School of Medicine, Johns Hopkins University, Baltimore, Maryland 21205*

Received 11 January 2008/Returned for modification 20 February 2008/Accepted 30 May 2008

**In exercise, as well as cancer and ischemia, hypoxia-inducible factor 1 (HIF1) transcriptionally activates hundreds of genes vital for cell homeostasis and angiogenesis. While potentially beneficial in ischemia, upregulation of the HIF1 transcription factor has been linked to inflammation, poor prognosis in many cancers, and decreased susceptibility of tumors to radiotherapy and chemotherapy. Considering HIF1's function, HIF1α protein and its hydroxylation cofactors look increasingly attractive as therapeutic targets. Independently, antioxidants have shown promise in lowering the risk of some cancers and improving neurological and cardiac function following ischemia. The mechanism of how different antioxidants and reactive oxygen species influence HIF1α expression has drawn interest and intense debate. Here we present an experimentally based computational model of HIF1α protein degradation that represents how reactive oxygen species and antioxidants likely affect the HIF1 pathway differentially in cancer and ischemia. We use the model to demonstrate effects on HIF1α expression from combined doses of five potential therapeutically targeted compounds (iron, ascorbate, hydrogen peroxide, 2-oxoglutarate, and succinate) influenced by cellular oxidation-reduction and involved in HIF1α hydroxylation. Results justify the hypothesis that reactive oxygen species work by two opposite ways on the HIF1 system. We also show how tumor cells and cells under ischemic conditions would differentially respond to reactive oxygen species via changes to HIF1α expression over the course of hours to days, dependent on extracellular hydrogen peroxide levels and largely independent of initial intracellular levels, during hypoxia.**

The transcription factor hypoxia-inducible factor (HIF) plays a critical role in the mammalian response to oxygen ($O_2$) levels. HIF1, the first characterized member of the HIF family, transcriptionally activates hundreds of genes associated with angiogenesis in cancer, exercise, and ischemia, as well as energy metabolism, nutrient transport, cell cycle, and cell migration (85, 98).

HIF1α and HIF1β make up the HIF1 heterodimer. The β-subunit is constitutively expressed in cells. Expression of the α-subunit may be induced by a number of pathways, and its degradation is highly sensitive to $O_2$ levels. Called a master switch for hypoxic gene expression (76, 85), intracellular HIF1α in normoxia is experimentally undetectable; during hypoxia, it rapidly accumulates in the cell nucleus and triggers gene expression. Molecular players involved in this process have come to light over the past 6 years; research has begun to define roles for prolyl hydroxylases, iron, ascorbate, hydrogen peroxide, 2-oxoglutarate, succinate, and von Hippel-Lindau protein in the HIF1 pathway.

Concomitantly, the study of reactive oxygen species (ROS) and the interest in antioxidants as potential dietary supplements for prevention of cancer, cardiac dysfunction, and neurodegeneration has grown rapidly. Ongoing debate surrounds the role of these compounds in hypoxic responses and the utility in pursuing them as preventative therapeutics. Some studies have shown increased ROS expression in hypoxia (10, 40), while others show a decrease (33, 96). Increased HIF1α expression has been found to contribute to mitochondrial activity (1), and specifically ROS formation, during hypoxia (26, 40, 81). However, other studies have demonstrated a decrease in HIF1α with increasing ROS (22, 99). Finally, some studies have shown no effects of $H_2O_2$ (87) or mitochondrial ROS in general (96). Related observations seem nearly as conflicting. Under hypoxic conditions, mitochondrial complex III may produce ROS, and the presence of high ROS concentrations generated from the mitochondria has been shown to stabilize HIF1α (8, 9, 20, 26). On the other hand, ROS may be produced in the cytosol, derived from NADPH oxidases (17, 33), and ROS may play a larger role in HIF1α expression during normoxia than hypoxia (43).

There are several hypotheses as to how ROS interact with the HIF1 pathway and alter HIF1α expression (recent related reviews include references 41 and 75). One possibility is that hydrogen peroxide oxidizes ferrous iron ($Fe^{2+}$) to its ferric form ($Fe^{3+}$), prohibiting the necessary binding of ferrous iron to the HIF1α hydroxylation enzymes, prolyl hydroxylases (PHDs) (71). Another change could be in the recruitment of ascorbate as a free radical scavenger, preventing ascorbate from reducing ferric iron and/or preventing ascorbate from binding directly to the PHDs. If ROS increased rather than decreased free $Fe^{2+}$, as suggested by some experiments, HIF1α hydroxylation would instead increase (56). Additionally, 2-oxoglutarate (2OG) and succinate (SC) are also compounds involved in HIF1α hydroxylation whose concentrations could be altered by free radicals and mitochondrial dysfunction (38, 56, 71). A fourth mechanism by which ROS could influ-

* Corresponding author. Mailing address: Department of Biomedical Engineering, School of Medicine, Johns Hopkins University, 613 Traylor Bldg, 720 Rutland Ave., Baltimore, MD 21205. Phone: (410) 955-1787. Fax: (410) 614-8796. E-mail: aqutub@jhu.edu.

† Supplemental material for this article may be found at http://mcb.asm.org/.

▽ Published ahead of print on 16 June 2008.

ence the HIF1 pathway is through changing the availability of oxygen to bind directly to the PHDs or changing PHD phosphorylation.

To address these alternate mechanisms and analyze possible competing factors involved in pro- and antioxidant therapy in cancer and ischemia, we developed a computational model describing the in vivo system and used it to observe dynamics currently inaccessible at the molecular level in vivo. Experimentally, ROS have been shown to affect the HIF1 pathway through changes in $H_2O_2$, $Fe^{2+}$, Asc, 2OG, or SC levels (61, 71), and mechanisms involving these compounds were the focus of this study.

The model consists of kinetic equations mapping the molecular steps in HIF1α degradation in normoxia, HIF1α synthesis in chronic hypoxia, and effects of the enzyme and cofactors involved in the HIF hydroxylation pathway. Kinetic values were estimated from in vitro studies, and results were validated by comparison to a series of independent experimental data. The input is cellular oxygen level, and the output is HIF1α levels in the nucleus in relation to necessary intermediate reactions, including reactions with prolyl hydroxylase, iron, 2-oxoglutarate, ascorbate, succinate, and von Hippel-Lindau (VHL) ligase. The model was expanded to represent two possible mechanisms of how ROS interact in the HIF1 pathway: (i) at high concentrations, ROS induce HIF1α by decreasing the activity of prolyl hydroxylases, and ROS effects can be silenced by antioxidants; (ii) in some cells with damaged mitochondria, the opposite effect (ROS decreasing HIF1 activity) is possible through increased iron and 2-oxoglutarate, cofactors in HIF1α degradation.

Using this model, we demonstrate how ascorbate, iron, hydrogen peroxide, 2-oxoglutarate, and succinate would alter HIF1α expression in two representative hypoxic microenvironments: cancer cells and cells during ischemia. We show how these compounds affect adaptation to chronic hypoxia, taking into account possible changes in succinate and reactive oxygen species levels associated with increased anaerobic metabolism and oxidative phosphorylation, such as those found in cancer. Results offer insight into the pro- and antioxidant effects of five compounds present in the HIF1 pathway and how they differ in a tumor microenviroment compared to ischemia. The model demonstrates temporal-specific molecular mechanisms that could be harnessed for use in cancer prevention, recovery from ischemic injury, and repression of angiogenesis and inflammatory signaling regulated by HIF1α expression.

## MATERIALS AND METHODS

**Formulation of the computational model.** A model of oxygen sensing by HIF1α was introduced and validated elsewhere (77). Here, we built an HIF1 computational model to incorporate potential mechanisms of ROS and antioxidants reacting within the HIF1α pathway. We represented ROS through two distinct means: (i) changes in the cofactors involved in HIF1α hydroxylation and (ii) the addition of hydrogen peroxide. The first mechanism is through direct increases or decreases in the concentration (availability) of certain cofactors of the hydroxylation pathway, i.e., by altering [$Fe^{2+}$], [Asc], and [2OG] levels, independent of $H_2O_2$ concentrations. The second mechanism focuses on $H_2O_2$ as a representative ROS and affects HIF1α hydroxylation through $Fe^{2+}$ and a Fenton reaction.

The complete model, based on an extensive analysis of experimental data, includes the hydroxylation of HIF1α by PHDs and the ubiquitination of hydroxylated HIF1α by VHL. Table 1 lists the compounds relevant to the current model. Equation 1 describes the overall scheme of HIF1α degradation. Equations 2 and 3 depict the oxidation of iron by reaction with hydrogen peroxide and the reduction of iron by ascorbate, respectively. The complete model includes HIF1α hydroxylation, independent reactions of iron and ascorbate, hydrogen peroxide production, succinate accumulation and product inhibition, PHD2 synthesis and HIF1α synthesis in chronic hypoxia, and the binding of HIF1α to VHL.

TABLE 1. Model variables and their abbreviations, as used in the paper

| Variable | Abbreviation |
|---|---|
| Concentration of A | [A] |
| Binding of A and B | A · B |
| Ascorbate | Asc |
| Iron | $Fe^{2+}$, $Fe^{3+}$ |
| Prolyl hydroxylase | PHD |
| Hypoxia-inducible factor | HIF1α |
| von Hippel-Lindau protein | VHL |
| Succinate | SC |
| Succinate dehydrogenase | SDH |
| Carbon dioxide | $CO_2$ |
| 2-Oxoglutarate | 2OG |
| Oxygen | $O_2$ |
| Hydrogen peroxide | $H_2O_2$ |
| Dehydro-ascorbate | 2dehydroAsc |
| Catalase | CA |
| Glutathione peroxidase | GPx |

The scheme of the overall biochemical reaction of HIF1α hydroxylation, with succinate product inhibition is as follows:

$$\mathrm{PHD2 + Fe^{2+} + 2OG + O_2 + Asc \leftrightarrow PHD2 \cdot Fe^{2+} \cdot 2OG \cdot O_2 \cdot Asc \leftrightarrow PHD2 + succinate + CO_2}$$
$$\mathrm{HIF1\alpha \quad HIF1\alpha_{hydroxylated}} \qquad (1)$$

Iron oxidation by reaction with hydrogen peroxide is depicted as follows:

$$\mathrm{Fe^{2+} + H_2O_2 \rightarrow Fe^{3+} + OH^{\cdot} + OH^{-}} \qquad (2)$$

Iron reduction by ascorbate (2, 101) is depicted as follows:

$$\mathrm{4Fe^{3+} + 2Asc + O_2 \rightarrow 2dehydroAsc + 4Fe^{2+} + 2H_2O} \qquad (3)$$

Enzyme-substrate binding kinetics are used to describe the hydroxylation reactions. Governing equations are determined from mass balances for the substrate and the intermediate enzyme-substrate complexes. A combination of enzyme-substrate saturation assumptions was used for the binding of iron, ascorbate, 2-oxoglutarate, and oxygen to PHD2, PHD2 hydroxylation of HIF1α, and VHL-mediated ubiquitination. In the hydroxylation reaction of PHDs with HIF1α, we represented the binding of PHD2 with the substrates iron, 2-oxoglutarate, and oxygen sequentially; the redox reactions for ascorbate and iron are included as separate equations (77). These hydroxylation steps and their output were validated against experiments previously (77, 78). Model inputs are initial compound concentrations, including cellular $O_2$ levels (Table 2). The output is HIF1α levels in the cell cytoplasm. The described kinetic model includes all previously studied reactions (77, 78).

Three feedback loops, HIF1 autocrine upregulation, HIF1 induction of PHD2, and succinate product inhibition, were determined to govern HIF1 levels and regulate the response to chronic hypoxia (Fig. 1) (78). Production terms were included for the synthesis of HIF1α and PHD2 at 3 and 4 h of hypoxia, respectively. The PHD2/HIF1α synthesis ratio is 0.01:0.05 in all cases presented in this paper; this ratio was chosen by estimating that between 4 and 8 hours there is a sixfold increase in HIF1α compared to initial conditions. $C_1$, a constant in the synthesis terms for PHD2 and HIF1α, was set at 0.1 (78).

The effects of succinate were represented by one of two mechanisms, as previously described (78). Briefly, product inhibition by succinate was included by modifying the backward kinetic rates for the PHD2 complex binding to unhydroxylated HIF1α. This inhibition could result from 2-oxoglutarate being converted into a succinic acid salt or succinate and therefore not allowing 2OG to be available to the PHD2 forward hydroxylation reaction. As an alternate possibility, succinate accumulation could trigger a change in PHD2 activity or HIF1α levels independent of product inhibition, through a yet-unknown signaling mechanism. A hypothesis is that succinate accumulation and related tricar-

TABLE 2. Parameters for the production and degradation of $H_2O_2$ in different microenvironments[a]

| Conditions | $[H_2O_2]_0$ (μM) | P[b] (μM/min) | $k_{catalase}$ [CA] ($min^{-1}$) | $k_{GPx}$ [GPx] ($min^{-1}$) | References |
|---|---|---|---|---|---|
| Normal | <1 ($10^{-3}$–0.7) | 0.19–0.45 | 40 ($k_{total}$) | | 4, 5, 18, 25, 37, 82, 88 |
| Tumor cell | 0.2 | 4.5–8.3 | 0[c]–8 | 246 | 5, 6, 19, 59, 90 |
| Ischemia | 0 | | 24 | 246 | 5, 32, 73 |
| Postischemia | | | | | |
| 0–30 min | | 0–0.19 | | | |
| 30–100 min | | 0.19–0.45 | | | |
| >100 min | | 0.73 | | | |
| Reperfusion | | | | | |
| 0–30 min | | 2.25 | | | |
| 30–210 min | | 2.25–0.0075 × $t$ | | | |
| >210 min | | 0.45 | | | |

[a] The values were experimentally determined or estimated. All values are at 37°C. $k_{catalase}$ [CA] and $k_{GPx}$ [GPx] are pseudo-first-order rate constants used to estimate the consumption of $H_2O_2$ by catalase (CA) and glutathione peroxidase (GPx), respectively, assuming constant concentrations of the enzymes. Values for the tumor and ischemic cells were approximated from experiments in disrupted Jurkat T cells (5) and data showing a two- to threefold decrease in catalase activity in cancer cells compared to noncancerous cells (59). See text for further details. $k_{total}$ refers to the total $H_2O_2$ intracellular consumption in intact cells and was also taken from experiments. $t$ is time, in minutes. The maximum value was used where there was a range, except for $[H_2O_2]_0$ for normal cells, which was set as 0.02 μM.

[b] $H_2O_2$ production rates measured for in vitro rat liver cell and subcellular extracts using a cytochrome $c$ peroxidase assay (18); the 0.45 μmol/min upper value refers to the initial rate found in cell homogenates, while the lower limit is estimated from adding up the $H_2O_2$ production from all measured subcellular compartments.

[c] The minimal value for the pseudo-first-order kinetic term of 0 $min^{-1}$ was estimated from experiments showing minimal concentrations of catalase in tumor cells (19).

boxylic acid (TCA) cycle changes correlate to a redistribution of intracellular oxygen or changes in oxygen demand. There is not yet experimental evidence to rule for or against this hypothesis about succinate's role; there is potentially related work on nitric oxide's involvement in intracellular oxygen redistribution (44) and structural evidence linking ROS and succinate dehydrogenase (45, 104) that leave this as a possibility to explore. One way of modeling this potential change is by altering the oxygen available for hydroxylation as a function of succinate production. In the figures shown below, we refer to the two mechanisms as "production inhibition" and "SC signals $O_2$ depletion."

In the present study, the model was expanded to include the production, transport, and metabolism of hydrogen peroxide, a representative ROS that is overproduced by mitochondria malfunction and during ischemic stress (Fig. 1). Here we only present equations not included in our previous work.

**Hydrogen peroxide.** Hydrogen peroxide is a reactive oxygen species that is also involved in the oxidation of $Fe^{2+}$, a cofactor in HIF1α hydroxylation (equation 3). Changes in the concentration of hydrogen peroxide were incorporated into the model by a mass balance to represent $H_2O_2$ production (either release from the cell mitochondria during hypoxia or NADPH oxidase-dependent $H_2O_2$ production), $H_2O_2$ degradation by glutathione peroxidase and catalase, and influx from the surrounding extracellular environment. $H_2O_2$ degradation and production were represented in all cell types through additional kinetic terms. The kinetic equation for hydrogen peroxide production and degradation is as follows:

$$\frac{d[H_2O_2]}{dt} = p - k_{catalase}[H_2O_2][\text{free catalase}] - k_{GPx}[H_2O_2][GPx] - k_{Fe3}[H_2O_2][Fe^{2+}] \quad (4)$$

where $p$ is a constant production term, estimated from experimental data in different microenvironments. This includes the oxidation of $Fe^{2+}$ by $H_2O_2$. $H_2O_2$ degradation is dependent on concentrations of catalase and glutathione peroxidase, GPx. Catalase is a mitochondrial enzyme that degrades $H_2O_2$ to water in

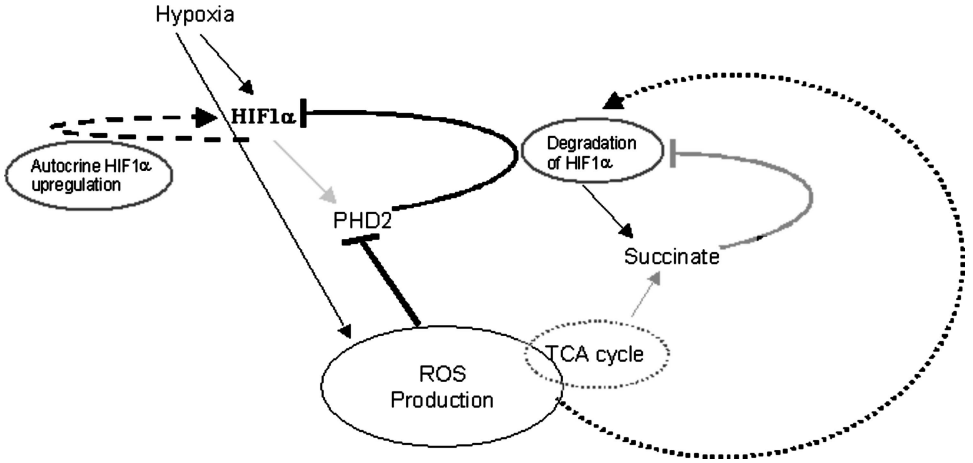


FIG. 1. Schematic of the HIF1α system during chronic hypoxia. Three feedback loops govern HIF1α hydroxylation: HIF1α synthesis (dashed line), PHD2 synthesis (light gray line), and succinate production inhibition (dark gray line). Succinate is also a metabolic product of the TCA cycle and is overproduced in some cancers. Two hypothesized, opposite effects of reactive oxygen species on HIF1α expression are shown: increasing HIF1α expression by blocking PHDs and decreasing HIF1α levels by signaling an increase in PHD activity and hydroxylation.

TABLE 3. Duration of hypoxia, hydrogen peroxide production, and estimated extracellular hydrogen peroxide in tumors and during ischemia[a]

| Condition | Hypoxic duration (h) | $H_2O_2$ production (beyond basal) | Extracellular $H_2O_2$[b] (μM) | Reference(s) |
|---|---|---|---|---|
| Tumor | >24 | >24 h, constant | 1.4 | 5 |
| Ischemia | >24 (if no reperfusion), 3 (if reperfusion[c]) | >100 min, with reperfusion beginning at 30 min, where used | 1.4, >14 (in reperfusion) | 58, 73 |

[a] Ischemia refers to endothelial cells under ischemic conditions.
[b] Extracellular hydrogen peroxide is estimated as a constant for each condition, with a large-enough pool of extracellular space to account for the changes due to $H_2O_2$ metabolized or produced by one cell. Experimental references helped provide reasonable $H_2O_2$ concentration ranges for different microenvironments. Under normal conditions, extracellular $H_2O_2$ is assumed to be in equilibrium with the intracellular concentrations, and $H_2O_2$ transport is not considered.
[c] Reperfusion is modeled with hypoxia (Fig. 6 and 7) and normoxia (see Fig. S3A and B in the supplemental material).

a catalytic reaction (and in a peroxidatic reaction, it degrades $H_2O_2$ in the presence of a hydrogen donor; here we consider only the catalytic reaction) (25). Glutathione peroxidase is a second enzyme that controls intracellular $H_2O_2$ levels, also by consuming $H_2O_2$ to produce water; unlike catalase, it is predominantly active in the cytosol. The kinetic rates $k_{catalase}$, $k_{GPx}$, and $k_{Fe3}$ are apparent first-order rates for a given initial $H_2O_2$ concentration. Table 2 provides the initial concentrations for $H_2O_2$ under different conditions, as well as estimates for the kinetic term $p$ and pseudo-first-order rate constants for the terms $k_{catalase} \times$ [free catalase] and $k_{GPx} \times$ [GPx]. $k_{Fe3}$ was estimated as $1.1 \times 10^{-2}$ $\mu M^{-1}$ $min^{-1}$ (12, 62). Table S1 in the supplemental material shows relative catalase and GPx activities for a number of cancer cell types, compared to noncancerous tissue. These values lend additional weight to the assumption that there is a threefold difference in catalase activity between tumor and noncancerous conditions (59).

To complete the representation of $H_2O_2$ intracellular concentration, possible diffusion of $H_2O_2$ into and out of the cell needs to be addressed. The $H_2O_2$ mass balance including transport is as follows:

$$\frac{d[H_2O_2]}{dt} = p - k_{catalase}[H_2O_2][\text{free catalase}] - k_{GPx}[H_2O_2][GPx] - k_{Fe3}[H_2O_2][Fe^{2+}] + \frac{p_{membrane} \cdot A}{V} \cdot ([H_2O_2]_{extracellular} - [H_2O_2]) \quad (5)$$

where $[H_2O_2]_{extracellular}$ is the extracellular concentration of hydrogen peroxide. The last term of equation 5 includes the change in $[H_2O_2]$ from the extracellular environment into the cell (units of $\mu M \cdot min^{-1}$), $\{(p_{membrane} \cdot A)/V\} \cdot [H_2O_2]_{extracellular}$ and $\{(p_{membrane} \cdot A)/V\} \cdot [H_2O_2]$, the outward $H_2O_2$ flux from the cell. Equal permeability is assumed for flux into the cell and flux out of the cell. From experimental analysis using T cells suspended in vitro, an estimate of the permeability coefficient for $H_2O_2$ across cell membranes, $p_{membrane}$, is $2 \times 10^{-4}$ $cm \cdot s^{-1}$. If the cells are represented as spheres with area $A$ of ~627 $\mu m^2$, radius of 7.5 μm, and volume $V$, then $p_{membrane} \cdot A/V \approx 0.8$ $s^{-1}$ or 48 $min^{-1}$ (5).

In representing nonischemic, noncancerous cells in vivo, where intracellular and extracellular $H_2O_2$ are at low levels, transport into and out of the cell is neglected, and the mass balance includes only production and metabolism (25), as in equation 4. For other conditions, including transport, the mass balance is given by equation 5. $H_2O_2$ diffuses rapidly, and for the current model, $H_2O_2$ concentration is represented as uniform throughout the cell.

**In vivo concentrations of $H_2O_2$.** While in vivo intracellular $H_2O_2$ concentrations in most cell types and in humans are not yet precisely known, estimates from measurements in bacteria and rat livers indicate levels on the order of 0.2 μM. In *Escherichia coli*, intracellular $H_2O_2$ concentrations were measured as 0.13 to 0.25 μM by one study (37) and estimated to be lower than 20 nM in the absence of exogenous sources in another study (82). Levels for mammalian cells range from $10^{-3}$ to $10^{-1}$ μM, depending on $H_2O_2$ production rates (25). Maximal $H_2O_2$ concentrations used for signaling in mammalian cells have been estimated as 0.5 to 0.7 μM (88). Variability among steady-state intracellular $H_2O_2$ in a single cell type is anticipated to be 50% or less (under different conditions of superoxide dismutase expression, relative steady-state intracellular $H_2O_2$ varied less than 20% in hamster lung fibroblasts [93]). However, it also should be noted that $H_2O_2$ concentrations can rise as high as 100 μM in phagocytes (72), and viable, transient levels of $H_2O_2$ in brain cells of >200 μM have been proposed (7).

The effects of added extracellular $H_2O_2$ have been studied in vitro by many research groups. As one example, extracellular $H_2O_2$ concentrations of 0.01 to 0.25 mM were shown to induce changes in characteristics of the potassium current in endothelial cells (higher concentrations of up to 0.5 mM had different effects on the potassium channel potential) (21). A transport model of $H_2O_2$ and experiments on $H_2O_2$ consumption indicate that following a change in $H_2O_2$, an equilibrium is reached within seconds between intracellular and extracellular $H_2O_2$ levels, with a 7- to 10-fold higher concentration in extracellular space, dependent on membrane permeability (5).

For the purposes of this study, initial in vivo intracellular concentrations of $H_2O_2$ were estimated from experiments, for normal physiology, as well as cancer and ischemic microenvironments (Table 2). For tumor cells, noncancerous (normal) cells, and noncancerous cells in ischemia, the default initial concentrations for $H_2O_2$ were 0.2 μM, 0.02 μM, and 0 μM, respectively. In the model, extracellular $H_2O_2$ is estimated as 1.4 μM, approximately sevenfold greater than the initial intracellular level for tumor and ischemic cells, and 14 μM during reperfusion (Table 3) (5, 88). Experimentally determined relative values for $H_2O_2$ kinetic parameters are provided in Table 5, below, for specific tumor types.

**Numerical solution.** The system of nonlinear differential equations was solved using Mathworks Matlab software. The ode23s solver, based on a modified Rosenbrock formula, was used to find a solution for the series of 19 differential equations. For the time integration, the solver used adjustable time steps with a default absolute error tolerance in the solution of $10^{-6}$ μM.

## RESULTS

**Tumor microenvironment.** The tumor microenvironment is predominantly associated with hypoxia, high rates of glycolysis, and high levels of reactive oxygen species. Furthermore, select enzymes that degrade ROS (e.g., catalase for $H_2O_2$) appear in lower levels in tumor-bearing mammals than in healthy ones (19, 25). Results of the model show effects of ROS on the HIF1α pathway in tumors through two proposed mechanisms: (i) direct changes in concentrations of the hydroxylation cofactors $Fe^{2+}$, Asc, and 2OG, or (ii) introduction of elevated levels of $H_2O_2$ and changes in $H_2O_2$ metabolism, production, and transport.

**ROS in tumors represented through $Fe^{2+}$, Asc, and 2OG.** Experiments suggest that ROS interact with the HIF1α pathway by altering the availability of $Fe^{2+}$ and Asc, hydroxylation cofactors (22, 34, 38, 54). The model showed effects of high ROS levels on a hypothetical microenvironment by changes in $Fe^{2+}$ and Asc levels (Fig. 2A). Where $[Fe^{2+}]_0$ and $[Asc]_0$ were upregulated, the peak amount of HIF1α occurred within the first hour, as in transient hypoxia (see Fig. S1A in the supplemental material). Without ROS and baseline levels of $Fe^{2+}$ and Asc, the model predicted a maximum in unhydroxylated HIF1α concentration near 4.5 h, whereas when ROS were represented by a decrease in $[Fe^{2+}]_0$ and $[Asc]_0$, the time to maximum HIF1α expression shifted by several hours, and HIF1α remained elevated over several days (Fig. 2A). Tenfold

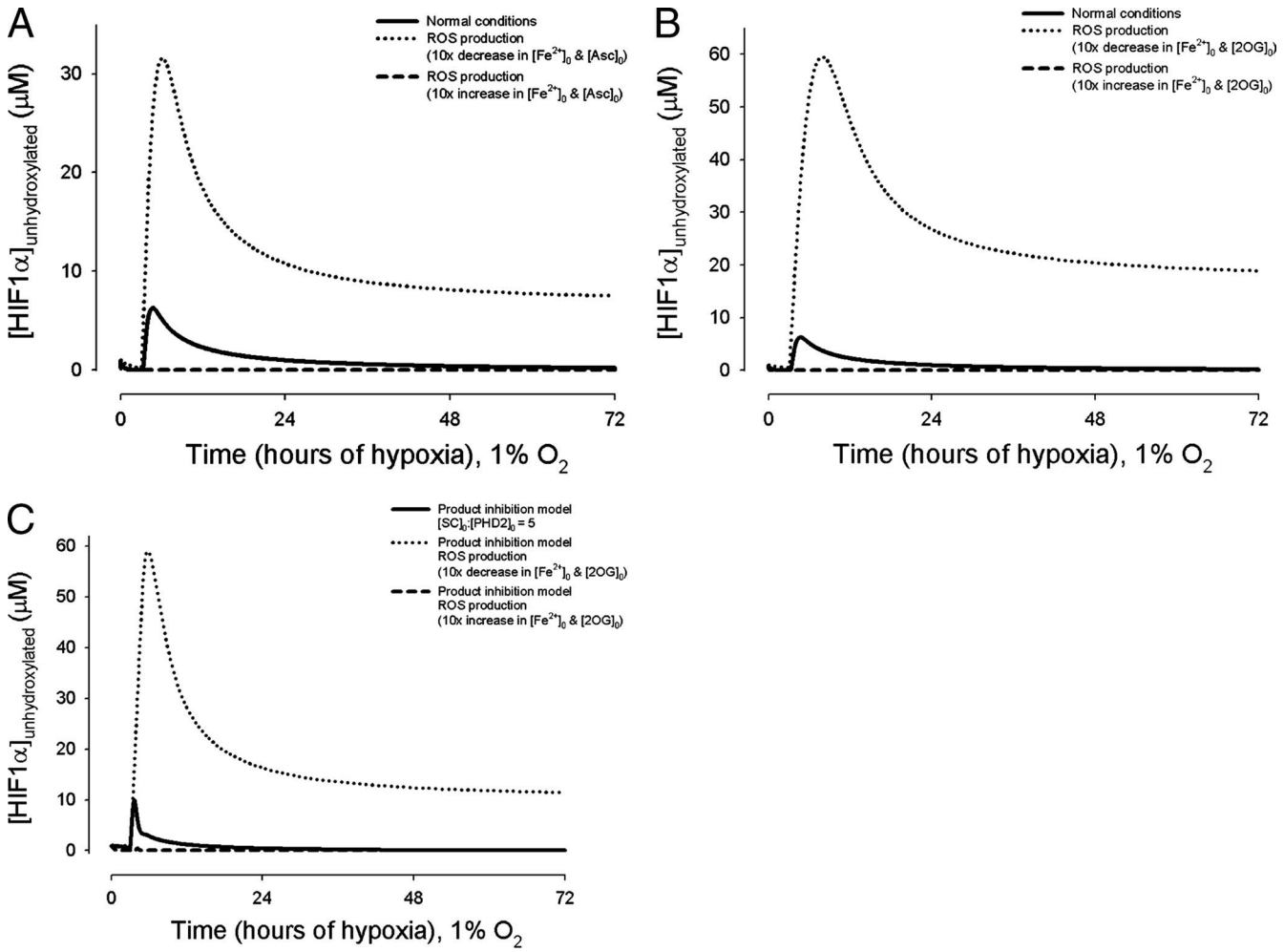


FIG. 2. HIF1α levels during chronic hypoxia are predicted for cells in the presence or (hypothetical) absence of ROS, where ROS is represented by changes in $Fe^{2+}$ and Asc or in $Fe^{2+}$ and 2OG concentrations. (A) HIF1α levels versus time in cells without SDH deficiency and the assumption of no succinate effect. ROS may be represented by a decrease (dotted line) or increase (dashed line) in $[Fe^{2+}]_0$ and $[Asc]_0$; the type and levels of ROS likely determine which mechanism is present (see Discussion). Figure S1A in the supplemental material provides a graph comparing normalized HIF1α levels for these conditions. (B) HIF1α levels versus time, where there is PHD2 hydroxylation production inhibition by succinate, with an initial concentration ratio of $[SC]_0$:$[PHD2]_0$ of 5. ROS is represented as a decrease in $[Fe^{2+}]_0$ and $[2OG]_0$ in this example (dotted line). Figure S1B and C in the supplemental material show the normalized and absolute HIF1α levels, respectively, for the conditions of $[SC]_0$:$[PHD2]_0$ of 500. For panels A and B, $[HIF1\alpha]_0 = 1$ μM.

decreases in $[Fe^{2+}]_0$ and $[Asc]_0$ led to an approximately fivefold increase in maximum HIF1α expression (Fig. 2A).

Other experiments indicate that $Fe^{2+}$ and 2-oxoglutarate are released by damaged mitochondria. 2-Oxoglutarate, like succinate, is a product of the citric acid cycle. In hypoxia, it has been hypothesized that nitric oxide causes mitochondrial dysfunction and thereby 2OG and $Fe^{2+}$ upregulation mediated by the reactive oxygen species peroxynitrite (56). Increased intracellular 2OG and $Fe^{2+}$ then contribute to increased hydroxylation of HIF1α by the PHDs. The model showed effects of high ROS levels on a hypothetical microenvironment by changes in $Fe^{2+}$ and 2OG levels (Fig. 2B).

**ROS in tumors with succinate effects.** Certain tumors, such as pheochromocytomas and paragangliomas, are associated with mitochondrial mutations and deficiencies in the enzyme succinate dehydrogenase (SDH). Succinate and 2-oxoglutarate are also intermediate products in the citric acid (TCA) cycle. In the hydroxylation reaction, PHD2 simultaneously splits oxygen to hydroxylate HIF1α and oxidizes and decarboxylates 2-oxoglutarate to succinate (83). Downregulation of SDH, an enzyme that degrades succinate to fumarate, leads to intracellular succinate accumulation, HIF1α stabilization, and HIF activation (83). Through in vitro and in vivo experimental observations, succinate was hypothesized to act as a product inhibitor of the PHD hydroxylation reaction of HIF1α (55, 74, 78, 83). Deciphering the relationship between succinate and ROS has been the subject of numerous studies, as well. Because of the structure of SDH redox centers, mutations in SDH have been predicted to result in ROS formation (104). Studies using both *Caenorhabditis elegans* (48, 86) and tumors with SDH mutations (49) have shown increased ROS. However, other studies have provided evidence that ROS is not necessary for succinate accumulation to produce a pseudo-hypoxic effect and stabilization of HIF1α (64, 74, 84). Shedding light on

TABLE 4. Initial concentrations for $O_2$, $Fe^{2+}$, Asc, SC, and 2OG for conditions represented in the model

| Condition[a] | $[O_2]_0$ (μM) | $[Fe^{2+}]_0$ (μM) | $[Asc]_0$ (μM) | $[2OG]_0$ (μM) | $[SC]_0$ (μM) | Reference(s) |
|---|---|---|---|---|---|---|
| Normal, hypoxia | 9.7 | 50 | 1,000 | 1,000 | 0 | 77 |
| Tumor (AF) | 9.7 | 5 | 100 | 1,000 | 0 | |
| Tumor (AF), SDH deficient | 9.7 | 5 | 100 | 1,000 | 500 | 53, 83 |
| Ischemia (AF) | 9.7 | 500 | $10^4$ | 1,000 | 0 | 22, 34, 38, 54[b] |
| Ischemia (OF) | 9.7 | 500 | 1,000 | $10^4$ | 0 | 56[b] |

[a] AF, ROS represented by $Fe^{2+}$ and ascorbate; OF, ROS represented by $Fe^{2+}$ and 2OG.
[b] The references showed the possibility of ROS up- or downregulating $Fe^{2+}$, Asc, or 2OG; the values are estimated examples.

both possibilities occurring under different conditions, recent research showed a link between mutations in particular subunits of mitochondrial complex II (succinate-ubiquinone oxidoreductase B [SdhB]), ROS production, and HIF1α activation, and no ROS connection with other complex II mutations (SdhA) (42). Another relevant study showed that SDH mutations could specifically contribute to tumor formation via both ROS production and a proliferative response associated with succinate accumulation (91). The computational model's predicted effect of ROS on tumors with SDH deficiency is shown in Fig. 2C; Table 4 shows the initial concentrations used to represent conditions found in vivo (78). ROS, represented by a 10-fold decrease in initial $Fe^{2+}$ and 2OG concentrations, shifted the time to the peak accumulation of HIF1α by several hours (Fig. 2B). The time to peak HIF1α accumulation was shifted up to ~48 h, when the model was used to represent in vitro conditions of succinate product inhibition (see Fig. S1B and C in the supplemental material; in these figures, $[SC]_0$ is 500 μM, the maximal concentration used to represent SDH deficiency in published in vitro experiments) (83). ROS, represented by a 10-fold decrease in initial $Fe^{2+}$ and Asc, also shifted the time to peak accumulation of HIF1α (see Fig. S1D in the supplemental material).

**ROS in tumors represented through $H_2O_2$.** The effect of ROS on HIF1α could be solely related to one ROS species, $H_2O_2$, its initial concentration, and its production in tumor cells (61). Measurements of $H_2O_2$ in vivo are difficult to obtain, and estimates for a base value of 0.2 μM in tumors were obtained from experiments, as described above. Fibroblasts that became tumorigenic with the expression of Nox1, the catalytic subunit of an NADPH oxidase, expressed $H_2O_2$ at a level 10-fold that of normal fibroblasts (6), in agreement with a number of studies that had established the relationship between increased $H_2O_2$ and tumorigenicity (24, 30, 90). Results from the model show the effect of an increase in initial $[H_2O_2]_0$, $H_2O_2$ production, and $H_2O_2$ metabolism predicted for a tumor cell (Fig. 3 and 4) and? a tumor cell with SDH deficiency represented by two distinct mechanisms (Fig. 4; see also Fig. S2 in the supplemental material). Additionally, the effects of extracellular $H_2O_2$ on HIF1α are predicted and compared to available in vitro experimental data (see Fig. S4 in the supplemental material).

**Ischemia microenvironment.** The ischemic microenvironment is associated with hypoxia, and high levels of reactive

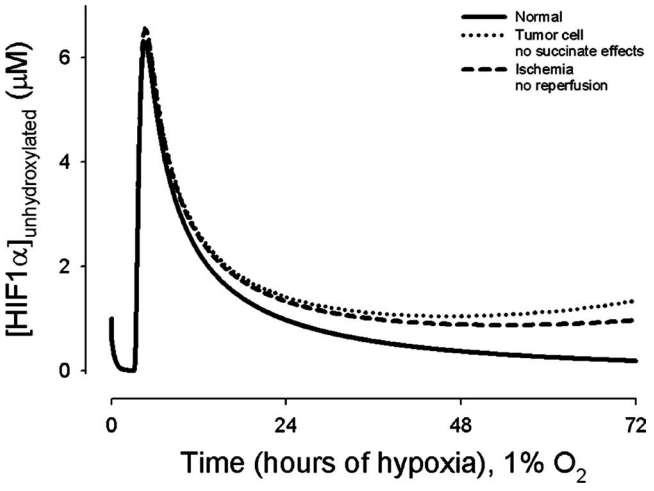


FIG. 3. Model results showing the effects of $H_2O_2$ on the cellular hypoxic response. HIF1α expression is predicted from 0 to 72 h for noncancerous (normal) cells, tumor cells, and cells exposed to ischemia. $[HIF1\alpha]_0 = 1$ μM. Both transient effects (PHD2 hydroxylation alone) before 3 h and chronic changes in hypoxia (PHD2 and HIF1α synthesis) are visible. Microenvironmental conditions correspond to those detailed in Table 2.

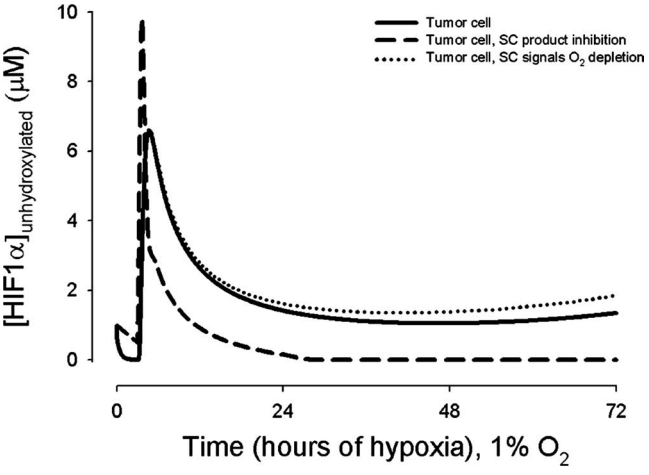


FIG. 4. Model results showing the effects of $H_2O_2$ on the cellular hypoxic response via HIF1α expression from 0 to 72 h in tumor cells and tumor cells with an SDH deficiency. $[HIF1\alpha]_0 = 1$ μM. Tumor cell conditions correspond to those detailed in Table 2. For the SDH tumors, the mechanism of succinate interaction was by inhibition of PHD2 hydroxylation (dashed line) or by succinate accumulation signaling a decrease in the amount of oxygen available for hydroxylation (dotted line). For both SDH deficiency conditions, $[SC]_0 = 5.0$ μM. $k_{SC} = 0.001\ min^{-1}$ for the case of succinate signaling oxygen depletion; for a further description, see equation A6 in reference 78.

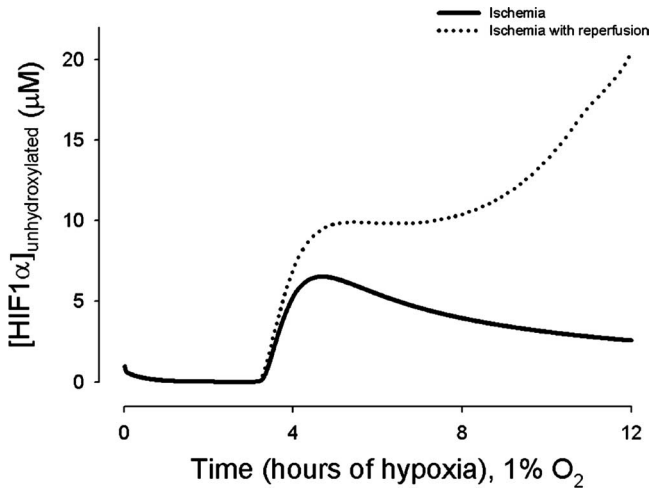


FIG. 5. Model results showing the effects of $H_2O_2$ on the cellular hypoxic response via HIF1α expression from 0 to 12 h in ischemic cells and ischemic cells exposed to ROS generated by reperfusion. Conditions correspond to those detailed in Table 2. $[HIF1\alpha]_0 = 1$ μM.

oxygen species are found both following the ischemic insult and during reperfusion.

**ROS in ischemia represented through $H_2O_2$.** The mechanism of ROS involvement in HIF1α expression during ischemia could be solely related to $H_2O_2$ initial concentrations and production. If this is the case, the model predicts a temporal expression of HIF1α in cells exposed to ischemia, similar to that of tumor cells (Fig. 3). This expression changes at the onset of reperfusion, which induces a larger amount of $H_2O_2$ production and alters $H_2O_2$ transport (Fig. 5; see also Fig. S4 in the supplemental material). If $H_2O_2$ extracellular levels remain elevated, the resulting increase in HIF1α lasts, uninhibited by any mechanism currently modeled, whether the intracellular conditions are approximated as hypoxia or normoxia (see Fig. S4 in the supplemental material).

**ROS in ischemia represented through $H_2O_2$, $Fe^{2+}$, and Asc or 2OG.** Using the ischemia microenvironment, a third and a fourth mechanism for how ROS affect the HIF1α pathway were tested, with increases in $H_2O_2$, Asc, and $Fe^{2+}$ or increases in $H_2O_2$, 2-oxoglutarate, and $Fe^{2+}$ simultaneously. The model results for changes in $Fe^{2+}$ and Asc or 2OG are shown, in conjunction with increased production of $H_2O_2$ (Fig. 6). In comparison to the $Fe^{2+}$ and Asc mechanism of ROS effects (a 10-fold increase in $Fe^{2+}$ and Asc) (Fig. 6A), an increase in 2OG accelerates the production of HIF1α and elevates its expression much higher by 8 h of hypoxia (Fig. 6B).

## DISCUSSION

The variable effects of ROS on HIF1α can be attributed to three main factors: (i) the degree of hypoxia, (ii) the form and intracellular location of ROS produced, and (iii) the molecular microenvironment of the cell. The third was the focus of this model. Before discussing the relevance of the microenvironment, it is worthwhile to briefly describe the roles of the first two factors, as they relate to the presented results.

**ROS, $O_2$ levels, and ROS species.** ROS production requires oxygen, so it is not surprising that ROS are expressed in different concentrations during anoxia, hypoxia, and normoxia. However, a direct correlation between ROS levels and $O_2$ availability remains elusive. Low $O_2$ limits formation of superoxide and its by-products (33), while hypoxia also has been shown to increase ROS, possibly through release by the mitochondria electron transport chain (41). Equally intriguing, ROS appear to play distinctly different roles in anoxia, hypoxia, and normoxia, with respect to the HIF1 system. In anoxia, the

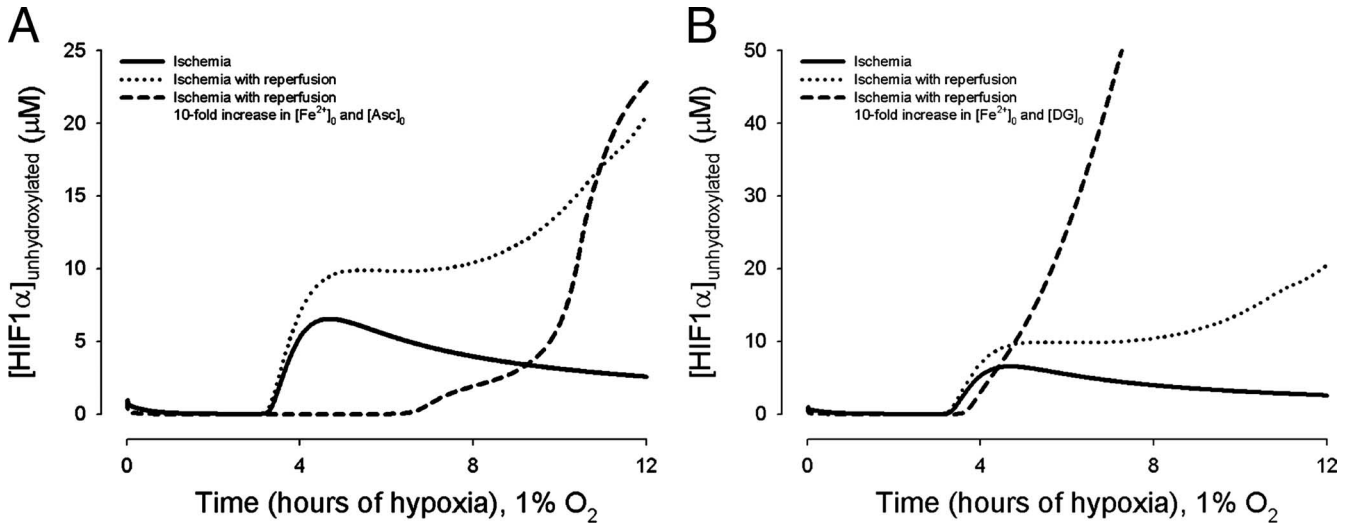


FIG. 6. Model results showing the effects of $H_2O_2$ on the cellular hypoxic response via HIF1α expression from 0 to 12 h in ischemic cells with reperfusion. (A) ROS is represented by both $Fe^{2+}$ and Asc increases and by $H_2O_2$ production (dashed line) and are compared to ROS represented just by $H_2O_2$ production (dotted line) and cells exposed to ischemia without reperfusion (solid line). See Fig. S3C in the supplemental material for an experiment under the same conditions, from 0 to 72 h. (B) ROS is represented by $Fe^{2+}$, 2OG, and $H_2O_2$ changes in ischemia (dashed line) and compared to ROS represented just by $H_2O_2$ production (dotted line) and cells exposed to ischemia without reperfusion (solid line). $[HIF1\alpha]_0 = 1$ μM.

electron transport chain in mitochondria may serve as oxygen sensor and regulator of HIF1α expression (41); as oxygen consumption by mitochondria becomes limited by $O_2$ availability only when $O_2$ falls below ~0.1%, mitochondria would not likely be an effective detector of moderate hypoxia. In hypoxia, some experiments suggest that at low or intermediate ROS concentrations induced by a superoxide generator, HIF1α is downregulated, as PHD activity is upregulated (22, 54). In related experiments, during normoxia, high ROS levels increased HIF1α, by blocking PHD hydroxylation. Additional studies have also indicated that in long-term hypoxia (12 h), the effect of ROS is to signal HIF1α degradation and downregulate HIF1α expression (27). In contrast, other experiments have shown in hypoxia that ROS upregulated HIF1α (6, 40, 75).

One explanation for the conflicting effects of ROS on HIF1α may be that HIF1α expression is dependent on particular reactive oxygen species, and not others (20); experiments differ in how they have measured ROS and in what cell types. ROS is produced by several means, which will affect ROS location and signaling. In normal cells, mitochondrial complex I and III and cytosolic monoamine and NADPH oxidases produce $H_2O_2$. In cancer cells, ROS, and $H_2O_2$ in particular, are additionally overproduced by mitochondrial respiration, while in ischemia, cells may be susceptible to ROS from both mitochondrial dysfunction and the extracellular environment, including effects of reperfusion injury. In both cases, inflammatory cells may also release ROS locally and affect intracellular levels in tumors and ischemic cells. Of all reactive oxygen species, $H_2O_2$ seems to be the one with the noticeable effect on the HIF1 system (20, 34, 61). However, the reactive oxygen species peroxynitrite may serve as an oxygen donor during HIF1α hydroxylation, as well as mediate $Fe^{2+}$ and 2OG release from the mitochondria (56, 89), and effects of superoxide on HIF1α have been shown in renal carcinoma (46) and renal medullary interstitial cells (103).

**Predictions: ROS and the cellular microenvironment.** The molecular environment, the focus of this work, distinguishes why the effects of ROS differ between tumor cells and ischemic cells. In tumor cells, the duration of hypoxia is generally longer, and the cell adapts to anaerobic metabolism and likely relatively stable levels of ROS production. HIF1α levels peak, as in normal cells, before 12 h (Fig. 4), and do not become elevated again until several days (see Fig. S3A in the supplemental material). In contrast, for the ischemic cell, the duration of ischemia is often hours or less, and cell is starved of oxygen but unable to adapt as readily as a cancer cell; additionally, the levels of ROS rapidly increase following the infarct or occlusion, and with perfusion, and then remain elevated for days, eventually decreasing (Fig. 5; see also Fig. S4A and B in the supplemental material).

**ROS mechanisms.** We represented the effects of ROS on the HIF1α through two different mechanisms: (i) altering the relative concentrations of cofactors in PHD2 hydroxylation of HIF1α and (ii) $H_2O_2$ production, transport, and metabolism. Both mechanisms involve the availability of free ferrous iron ($Fe^{2+}$), a cofactor in the hydroxylation reaction, via a mechanism that has been shown in experiments (34). They differ in that the first mechanism was modeled by changing the availability of $Fe^{2+}$ and Asc (Fig. 2A and 6A) or $Fe^{2+}$ and 2OG (Fig. 2B and C and 6B), while $H_2O_2$ only altered the availability of free ferrous iron in the model. Changes in $H_2O_2$ concentration were highly dependent on the microenvironment (Tables 2 and 3).

The results from the model lend credence to the hypothesis that ROS interacts with the HIF1 system through several different mechanisms, and they may help explain conflicting experiments on HIF1α expression and ROS (Table 5). If ROS work by both increasing $Fe^{2+}$ and Asc or 2OG (Fig. 2 and 6) and increasing $H_2O_2$ (thereby decreasing free $Fe^{2+}$) (Fig. 3, 4, and 5), depending on the hypoxic conditions, then there could be a dual effect of ROS so that in some cases it upregulates HIF1α and in others it downregulates it. Moreover, in the first mechanism, $Fe^{2+}$, Asc, and 2OG are quickly depleted in ischemic-reperfusion conditions, and the relatively lower HIF1α level is a transient effect (Fig. 6). Beyond 5 to 12 h (with a 10-fold increase in 2OG and Asc, respectively), HIF1α levels reach the same level or higher, as they do using $H_2O_2$ alone to represent ROS (Fig. 6; see also Fig. S4B and C in the supplemental material). Depending on the duration of hypoxia in experiments, the model then predicts the same ROS conditions would yield either a relative upregulation or downregulation of HIF1α. Model results using $H_2O_2$ as the representative ROS are in agreement with experimental studies showing $H_2O_2$ depletes ascorbate (70) (data not shown). The effect of an infinite source of Asc and free $Fe^{2+}$ has not yet been measured experimentally or modeled with respect to the HIF1α system and ROS; this would be an interesting test of altering hypoxic response through nutritional supplementation.

**ROS in cancer and in ischemia. (i) $H_2O_2$ in cancer.** Restricting the effect of the ROS in the model to changes in $H_2O_2$ levels offers insight into how differences in cancer and ischemic microenvironments determine distinct cell fates. The effects of $H_2O_2$ on the HIF1α concentrations are dependent on the dose of $H_2O_2$, levels of hypoxia, and cell type. Seemingly contradictory, high levels of $H_2O_2$ are associated not only with the progression of cancer to metastasis but also the susceptibility of cancer cells to cell death (61). An existing hypothesis to explain this observation is that all cells, cancer cells included, have an upper threshold for $H_2O_2$ concentration, above which apoptosis occurs and below which cells proliferate at a rate proportional to the amount of $H_2O_2$ (36, 59) (Fig. 7). The model predicts cancer cells reach a lower steady-state level of $H_2O_2$ than cells exposed to ischemia and reperfusion (Fig. 8). Assuming the threshold hypothesis is true, the model implies cancer cells are more apt to survive in their hypoxic microenvironment well beyond the survival time of cells exposed to ischemia-reperfusion, at the same duration of hypoxia.

Additionally, HIF1α expression is increasing as $H_2O_2$ increases or remains elevated below the threshold (Fig. 7), making the cancer cells more virile and less susceptible to radiation and chemotherapy (50). Increased HIF1α expression triggers the production of angiogenic factors in both cancer and ischemic cells, but the ischemic cells have less of a chance to survive their high intracellular ROS levels, while angiogenesis fuels the cancer cells' proliferation. If ROS works through an increased $Fe^{2+}$, Asc, or 2OG mechanism too, the time to peak HIF1α levels is delayed (Fig. 2 and 6; see also Fig. S1 in the supplemental material), potentially delaying the onset of an-

TABLE 5. Experiments showing the up- or downregulation of HIF1α under different conditions explored in the model[a]

| Condition | Cell line or tissue | ROS | HIF1α regulation | | Reference |
|---|---|---|---|---|---|
| | | | Protein | mRNA | |
| Normoxia, noncancerous | BAEC | $O_2^{\cdot-}$ | — | ↑ | 31 |
| | hcVSMC | $O_2^{\cdot-}$ | ↓ | NM | 100 |
| | HEK293 | ROS from complex III | ↑ | NM | 40 |
| Hypoxia, noncancerous | HEK293 | ROS from complex III | ↑ | NM | 20 |
| | HEK293 | Endogenous multiple ROS | — | NM | 44 |
| | HEK293 | Endogenous multiple ROS | ↑ | NM | 66 |
| | hcVSMC | $O_2^{\cdot-}$ | ↓ | NM | 100 |
| Cancer | A549 | Exogenous $H_2O_2$ (500 μM, 1 h) | ↑ | NM | 52 |
| | A549 | Endogenous $H_2O_2$ | ↑ | NM | 20 |
| | A549 | $O_2^{\cdot-}$ | — | NM | 20 |
| | OVCAR-3 | Endogenous $H_2O_2$ | ↑ | NM | 102 |
| | OVCAR-3 | $O_2^{\cdot-}$ | — | NM | 102 |
| | HeLa | Exogenous $H_2O_2$ (500 μM, 1 h) | ↑ | NM | 52 |
| | HCT116 | Exogenous $H_2O_2$ (500 μM, 1 h) | ↑ | NM | 52 |
| | HepG2 | Exogenous $H_2O_2$ (500 μM, 1 h) | ↑ | NM | 52 |
| | HepG2 | Endogenous multiple ROS | ↓ | NM | 22 |
| | Hep3B | Exogenous $H_2O_2$ (300 and 1,000 μM, 1 h) | ↑ | — | 71 |
| | Hep3B | Exogenous $H_2O_2$ (25, 50, and 100 μM, 1 and 2 h) | ↑ | NM | 66 |
| | HT1080 | Endogenous multiple ROS | — | NM | 94 |
| | DU-145 | Exogenous $H_2O_2$ (0–1,000 μM, maximum HIF1α at 0.5 mM; 0–12 h, maximum HIF1α at 0.5–4 h with 0.5 mM) | ↑ | NM | 52 |
| | DU-145 | Endogenous multiple ROS; exogenous $H_2O_2$ | ↓ | NM | 99 |
| | RT1 | Exogenous $H_2O_2$ (5, 10, or 25 μM, every 20 min for 10 h) | ↑ | NM | 68 |
| | U251 | Exogenous $H_2O_2$ (20 and 40 μM, 4 h) | ↑ | NM | 63 |
| Ischemia | Whole rat brain | Not assessed | ↑, 20 h after occlusion | ↑↑, starting 4 to 7 h after occlusion to 20 h | 13 |

[a] NM, not measured in the study; —, no significant change.

giogenesis. Furthermore, there may be a threshold for maximum HIF1α levels like that hypothesized for $H_2O_2$ levels, above which apoptosis occurs, in which case, again the cells exposed to ischemia-reperfusion would be more susceptible than cancer cells (Fig. 7B). In support of the model's prediction of extracellular $H_2O_2$ effects on HIF1 in cancer cells, results were compared to experimental data looking at in vitro conditions where cancer cells were supplemented with $H_2O_2$

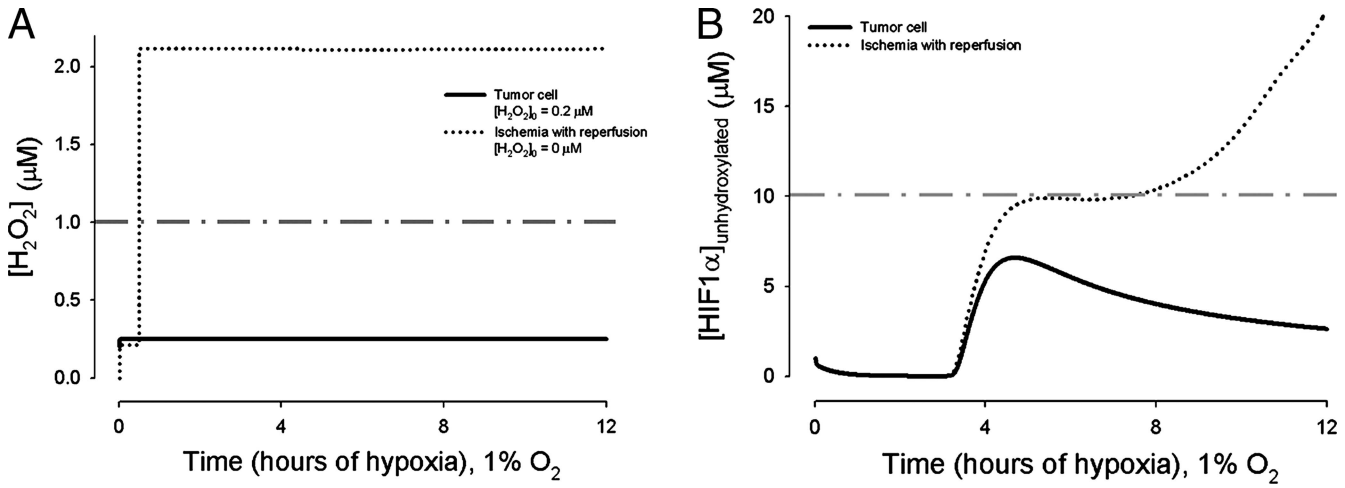


FIG. 7. Potential effects of the threshold hypothesis. Thresholds are represented by the horizontal dashed-dotted lines. (A) If intracellular levels of $H_2O_2$ above ~1 μM induced apoptosis (4), cells exposed to ischemia-reperfusion injury would die within an hour, while cancer cells would survive. (B) If a hypoxic response and/or apoptosis were also contingent on threshold HIF1α expression (10 μM is shown as an example), ischemia-reperfusion cells could again be more susceptible than cancer cells.

and insulin. While no direct comparison can be made, as the conditions are not the same and the experiment assessed HIF1 activity through hypoxic gene activation, the trend of increasing HIF1 activity and then saturation at high extracellular $H_2O_2$ agree (see Fig. S4 in the supplemental material).

**(ii) $H_2O_2$, ischemia, and reperfusion.** Along with differentiating the effects of ROS in cancer cells and cells exposed to ischemia, the model results shed light on two additional experimental observations: concentration-dependent effects of $H_2O_2$ and the extent of reperfusion injury. The model described $H_2O_2$ concentration as a function of production, transport, and metabolism. The intracellular concentration of $H_2O_2$ (high or low) rapidly reaches an equilibrium level dependent on extracellular concentrations. This is a function of its quick transport across the cell membrane (5, 16), combined with the driving force of intracellular metabolism (see Fig. S2B and S3D in the supplemental material). As a consequence of the rapid equilibrium, initial concentrations of $H_2O_2$ are of minimal relevancy, and the model predicts that sustained intermediate levels of intracellular $H_2O_2$ have the most significant effect on increasing HIF1α expression in tumors and ischemia and altering the hypoxic response long term (Fig. 7A). While there may be many explanations other then sustained, elevated intracellular $H_2O_2$ levels, this conclusion also offers an interesting perspective on experimental evidence showing that intermediate $H_2O_2$ levels produce more DNA lesions than higher or lower $H_2O_2$ concentrations (69) and supports experiments showing some cells can fully recover from transient very high levels of $H_2O_2$ (7).

The model predicts reperfusion produces a far greater increase in $H_2O_2$-dependent HIF1α expression than ischemia alone (Fig. 5), even while $H_2O_2$ production decreases to normal levels with reperfusion after 3.5 h (Table 2). This is true even if reperfusion is considered to provide enough oxygen for cells to reach normoxia (see Fig. S3A and B in the supplemental material). Anticipated high extracellular levels of $H_2O_2$ during reperfusion drive this elevated $H_2O_2$-dependent HIF1α (Table 3).

The model then highlights how regulating hydrogen peroxide temporally is essential in treatments for ischemia-reperfusion injury. In vivo, high oxidant stress following ischemia may drive angiogenesis, allowing recovery of normoxia through the growth of vessels, while on the other hand too high levels of oxidants damage tissues. Modeling is key to correctly pinpointing the effective time frame for therapeutics, and as the computational modeling advances with new experimental and clinical measurements, antioxidant and proangiogenic treatments could be tailored to individuals.

**Metabolism of ROS: catalase, GPx, and variability.** In experiments using human hepatoma cells, catalase overexpression did not show an appreciably different effect on HIF1 expression or transcriptional activity (87). The opposite has been shown in other cell types (20). The authors of the first study suggested that $H_2O_2$ played little or no role as a signaling molecule in the hypoxic response. As another possibility, which could explain discrepancies between studies, $H_2O_2$ may play a role in HIF1 activation only or predominantly in hypoxia, but not anoxia (81). Our model suggests a third explanation. An increase in intracellular catalase concentration does not have a strong effect on the hypoxic response via direct HIF1 activation, while extracellular $H_2O_2$ and catalase levels do. Lending support to the model's finding that extracellular $H_2O_2$ greatly determines the cellular hypoxic response, recent studies have indicated catalase added to cell medium has a strong effect on cell-cell communication in microglia via NO signaling (47). Furthermore, another study showed that an adenovirus containing catalase affected the activity of apoptosis signal-regulating kinase 1, another signaling molecule involved in hypoxia and ischemia, whose activity is dependent on $H_2O_2$ and indirectly related to HIF1 (57).

The model offers plausible mechanisms to explain several phenomena associated with ROS effects on the HIF1 system; however, it is worthwhile to mention limitations of the current model. In vivo intracellular $H_2O_2$ concentrations depend on a number of parameters that vary by cell type. These parameters include the concentration and activities of the peroxisome enzyme catalase and glutathione peroxidase, predominant in the cell cytosol; both enzymes degrade $H_2O_2$ into water. The concentrations and activities of these enzymes were approximated as constants in the model (Table 2), and further studies would represent how known changes in their activities affect intracellular $H_2O_2$ concentrations and the HIF1 system. For example, the concentration of catalase is known to vary with cell type, ranging from 4 ng/$10^6$ cells in lymphocytes to 850 ng/$10^6$ cells in macrophages (80). The variability among endothelial cells is expected to be less; however, it has not been established experimentally to our knowledge (in bacteria, a variability in catalase activity of 10- to 20-fold has been assessed [79]). Studies measuring tissue-level catalase activity lend weight to the model's assumption of constant catalase activity during ischemia and reperfusion (39). However, the concentration and activity of intracellular catalase, as well as the scavenging enzyme GPx, are likely specific to the cell and tissue type, as well as age (67) (see Fig. S1 in the supplemental material). $H_2O_2$ membrane transport has been modeled here as unlimited diffusion (65), while facilitated transport by aquaporins may also occur (15). Additionally, extracellular $H_2O_2$ is estimated as a constant for each condition considered in the model. When more observations become available on the temporal changes in extracellular $H_2O_2$ during cancer and ischemia, it would be interesting to include effects of changing local extracellular $H_2O_2$.

The model predicts that in tumors, the metabolism of $H_2O_2$ drives increased transport from the extracellular microenvironment, while $H_2O_2$ production by a single cell is a fraction of what is being metabolized (see Fig. S3D in the supplemental material). The model approximated uniform metabolism and production throughout the cell, while production occurs in subcellular units or areas of the cytoplasm. As another consideration, the transport of $H_2O_2$ into and out of the cell and intracellular membranes (i.e., peroxisomes) affects the $H_2O_2$ gradients present in the cell. How the response to an isolated, high concentration of ROS differs from a cell's response to uniform intracellular ROS elevation merits exploration.

Another characteristic of the model suggests an avenue for experimental pursuit. The current model has no specific feedback on ROS effects. Model predictions for HIF1α accumulation in chronic conditions correlate well with a range of experiments showing a peak in HIF1α before 12 h (Fig. 3; see also Fig. S2A in the supplemental material). However, without a

way to negatively regulate ROS, for hypoxic and ischemic durations beyond 48 h, the model predicts elevated HIF1α levels that have not been seen in many experiments (see Fig. S2A and S3B and Table S2 in the supplemental material). Potential sources of adaptation to ROS or downregulation of ROS effects on HIF1α could be changes in PHD2 activity or $O_2$ redistribution.

**A systems view of HIF1α signaling.** As HIF1 is a transcription factor, its protein regulation is interesting in the greater context of systems biology. From experiments and computational modeling thus far, in chronic hypoxia HIF1α has two positive autoregulatory feedback mechanisms, HIF1α upregulating itself and the hydroxylation product succinate downregulating PHD2 to upregulate HIF1α, and one negative one, HIF1α-dependent upregulation of PHD2 (78). Furthermore, ROS regulates HIF1α expression; this provides another form of autocrine regulation by a hypoxic cell.

What does a hypoxic cell gain from these multiple regulatory pathways, both negatively and positively? Negative autoregulation alone speeds the response time for a closed regulatory circuit and leads to saturation in the protein. If HIF1α only regulated PHD2, and not itself, this would be the expected result; on the other hand, if HIF1α regulated HIF1α alone and not PHD2, the positive feedback would lead to a slower response time and could lead to indefinitely increasing HIF1α conditions. From experiments, HIF1α auto-upregulation occurs an hour or more prior to HIF1α-dependent PHD2 upregulation. One might expect from this a characteristic peak found in HIF1α expression, with a chronic decay rate of HIF1α dependent on the synthesis ratio of PHD2:HIF1α (78). The staggered response coupling both positive and negative feedback then potentially optimizes both the degree of HIF1α upregulation and the speed of its regulation during periods of chronic hypoxia.

HIF1α protein regulation during hypoxic durations of less than 3 hours is modulated without feedback. This provides a response within minutes (HIF1α accumulation in hypoxia and HIF1α oxygen-dependent degradation). There is no need to keep the response on, once oxygen is restored. It may also be that some genes are upregulated by HIF1 specifically during long-term hypoxia, and the concentration or duration of the transient HIF1 response is insufficient to trigger their activation.

To summarize and weigh current hypotheses on ROS at a systems level, a brief network motif analysis of possible ROS mechanisms in regards to HIF1 and hypoxia is presented (Fig. 8). Figure 8 provides circuit representations of hypotheses of ROS and HIF1α interactions. A coherent feed-forward loop refers to a circuit where the indirect path and the direct path yield the same response; an incoherent loop refers to one where the two paths cause opposite effects (3). Of the three proposed mechanisms of ROS, the incoherent feed-forward type 1 (Fig. 8B), is one of the most prevalent circuits in biological systems, albeit at the gene level (3). In this case ROS may increase HIF1α through limiting $O_2$ availability, ferrous iron, and Asc or decrease HIF1α by increasing 2OG and $Fe^{2+}$ or donating $O_2$ in hypoxia, all cofactors in PHD2 hydroxylation. If ROS mechanisms can be described by this circuit, pulse-like dynamics in HIF1α expression may be possible; ROS would begin to upregulate HIF1α independently of PHD2 and then PHD2 would be upregulated by ROS, leading to HIF1α downregulation (3). Other possible mechanisms of ROS interactions are shown, as well as the effects of succinate and hypoxia globally on HIF1α. At the transcriptional level, these configurations are rarer than the incoherent feed-forward type 1, and they are characterized by limited function.

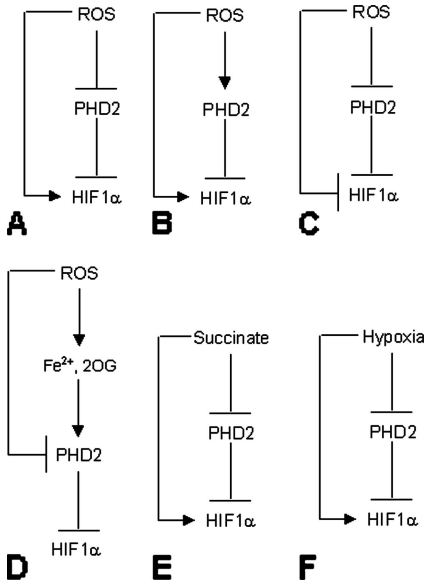


FIG. 8. Circuit representations of ROS effects on the HIF1α pathway. (A) Coherent feed-forward loop type 4 in hypoxia, where ROS blocks PHD2 expression, leading to upregulation of HIF1α; another upregulation of HIF1α by ROS may come as a direct dependency of oxygen availability. (B) Incoherent type 1 feed-forward loop, where ROS may increase HIF1α through limiting $O_2$ availability, ferrous iron, and Asc or decrease HIF1α by increasing 2OG and $Fe^{2+}$ or donating $O_2$ in hypoxia. (C) Incoherent type 2 feed-forward loop, where ROS blocks HIF1α through PHD2 or independently by donating $O_2$ in hypoxia. (D) Incoherent type 3 feed-forward loop, where ROS increases 2OG and $Fe^{2+}$ or, conversely, blocks PHD2. (E) Succinate follows a coherent type 4 mechanism to increase the HIF1 response by blocking PHD2 or possibly by independently signaling a limitation in $O_2$ availability. (F) A coherent type 4 loop can describe the effects of hypoxia on HIF1α, through PHD2-dependent and $O_2$-independent mechanisms (e.g., the AKT pathway).

If the prevalence of specific motifs at the transcriptional level can be extrapolated to molecular species and proteins, the presented circuit analysis helps support the hypothesis from the molecular model that ROS acts by both up- and downregulating HIF1, rather than one or the other. The allure of representing the system in circuit diagram form is both enhanced and tempered by the known biological complexity of the HIF1 system. In graphical form, hypothesized positive and negative controls on HIF1 become simplified; adding components, e.g., metabolic pathways, becomes relatively easy. However, even while highlighting characteristics of simple circuits and network motifs, the interactions, delay time, protein versus gene response, and multiple connections can alter the excepted benefits or characteristics of a particular motif.

The presented model demonstrates several molecular mechanisms for how ROS signaling can affect the HIF1 pathway through $Fe^{2+}$, Asc, 2OG, SC, and $H_2O_2$. We showed how tumor cells and cells exposed to ischemia would differentially

respond to ROS via changes to HIF1α expression over the course of hours to days. Model results also show that in hypoxia (both in cancer and ischemic microenvironments), $H_2O_2$ intracellular levels rapidly reach equilibrium with extracellular levels, largely independent of initial intracellular levels. $H_2O_2$ transport and metabolism, more than cellular production, dictate HIF1α levels. Antioxidants (e.g., Asc) can alter the amount of ROS that is metabolized intracellularly and restore free $Fe^{2+}$ levels, but unless the extracellular ROS levels change too, this effect is transient. Applied to therapeutic manipulation of hypoxic response, model results imply that antioxidants would need to be applied judiciously at the correct intervals (a sustained, moderate level) to have a noticeable effect on HIF1α levels either in the cancer or ischemic-reperfusion microenvironment. The optimal concentration would be dictated by the hypoxic microenvironment, and the model suggests noticeably higher doses would be needed to avoid reperfusion injury than those needed to prevent cancer cell proliferation or reduce ischemic damage alone.

## ACKNOWLEDGMENTS

This work was supported by NIH 1F32HL085016-01 (A.Q.) and NIH HL079653 and NIH HL087351 (A.S.P.).

We thank J. Pouyssegur for useful discussions.

## REFERENCES

1. **Agani, F. H., P. Pichiule, J. C. Chavez, and J. C. LaManna.** 2000. The role of mitochondria in the regulation of hypoxia-inducible factor 1 expression during hypoxia. J. Biol. Chem. **275:**35863–35867.
2. **Al-Ayash, A. I., and M. T. Wilson.** 1979. The mechanism of reduction of single-site redox proteins by ascorbic acid. Biochem. J. **177:**641–648.
3. **Alon, U.** 2007. An introduction to systems biology. Chapman & Hall, Boca Raton, FL.
4. **Antunes, F., and E. Cadenas.** 2001. Cellular titration of apoptosis with steady state concentrations of $H_2O_2$: submicromolar levels of $H_2O_2$ induce apoptosis through Fenton chemistry independent of the cellular thiol state. Free Radic. Biol. Med. **30:**1008–1018.
5. **Antunes, F., and E. Cadenas.** 2000. Estimation of $H_2O_2$ gradients across biomembranes. FEBS Lett. **475:**121–126.
6. **Arnold, R. S., J. Shi, E. Murad, A. M. Whalen, C. Q. Sun, R. Polavarapu, S. Parthasarathy, J. A. Petros, and J. D. Lambeth.** 2001. Hydrogen peroxide mediates the cell growth and transformation caused by the mitogenic oxidase Nox1. Proc. Natl. Acad. Sci. USA **98:**5550–5555.
7. **Avshalumov, M. V., L. Bao, C. P. J., and M. E. Rice.** 2007. $H_2O_2$ signaling in the nigrostriatal dopamine pathway via ATP-sensitive potassium channels: issues and answers. Antioxid. Redox Signal. **9:**219–231.
8. **Bell, E. L., and N. S. Chandel.** 2007. Mitochondrial oxygen sensing: regulation of hypoxia-inducible factor by mitochondrial generated reactive oxygen species. Essays Biochem. **43:**17–27.
9. **Bell, E. L., T. A. Klimova, J. Eisenbart, C. T. Moraes, M. P. Murphy, G. R. Budinger, and N. S. Chandel.** 2007. The Qo site of the mitochondrial complex III is required for the transduction of hypoxic signaling via reactive oxygen species production. J. Cell Biol. **177:**1029–1036.
10. **Bell, E. L., T. A. Klimova, J. Eisenbart, P. T. Schumacker, and N. S. Chandel.** 2007. Mitochondrial reactive oxygen species trigger hypoxia-inducible factor-dependent extension of the replicative life span during hypoxia. Mol. Cell. Biol. **27:**5737–5745.
11. **Bellisola, G., M. Casaril, G. B. Gabrielli, M. Caraffi, and R. Corrocher.** 1987. Catalase activity in human hepatocellular carcinoma (HCC). Clin. Biochem. **20:**415–417.
12. **Beltran, F. J., M. Gonzalez, F. J. Rivas, and P. Alvarez.** 1998. Fenton reagent advanced oxidation of polynuclear aromatic hydrocarbons in water. Water Air Soil Pollut. **105:**685–700.
13. **Bergeron, M., A. Y. Yu, K. E. Solway, G. L. Semenza, and F. R. Sharp.** 1999. Induction of hypoxia-inducible factor-1 (HIF-1) and its target genes following focal ischaemia in rat brain. Eur. J. Neurosci. **11:**4159–4170.
14. **Bernaudin, M., A. S. Nedelec, D. Divoux, E. T. MacKenzie, E. Petit, and P. Schumann-Bard.** 2002. Normobaric hypoxia induces tolerance to focal permanent cerebral ischemia in association with an increased expression of hypoxia-inducible factor-1 and its target genes, erythropoietin and VEGF, in the adult mouse brain. J. Cereb. Blood Flow Metab. **22:**393–403.
15. **Bienert, G. P., A. L. Moller, K. A. Kristiansen, A. Schulz, I. M. Moller, J. K. Schjoerring, and T. P. Jahn.** 2007. Specific aquaporins facilitate the diffusion of hydrogen peroxide across membranes. J. Biol. Chem. **282:**1183–1192.
16. **Bienert, G. P., J. K. Schjoerring, and T. P. Jahn.** 2006. Membrane transport of hydrogen peroxide. Biochim. Biophys. Acta **1758:**994–1003.
17. **Biswas, S., M. K. Gupta, D. Chattopadhyay, and C. K. Mukhopadhyay.** 2007. Insulin-induced activation of hypoxia-inducible factor-1 requires generation of reactive oxygen species by NADPH oxidase. Am. J. Physiol. Heart Circ. Physiol. **292:**H758–H566.
18. **Boveris, A., N. Oshino, and B. Chance.** 1972. The cellular production of hydrogen peroxide. Biochem. J. **128:**617–630.
19. **Bozzi, A., I. Mavelli, B. Mondovi, R. Strom, and G. Rotilio.** 1981. Differential cytotoxicity of daunomycin in tumour cells is related to glutathione-dependent hydrogen peroxide metabolism. Biochem. J. **194:**369–372.
20. **Brunelle, J. K., E. L. Bell, N. M. Quesada, K. Vercauteren, V. Tiranti, M. Zeviani, R. C. Scarpulla, and N. S. Chandel.** 2005. Oxygen sensing requires mitochondrial ROS but not oxidative phosphorylation. Cell. Metab. **1:**409–414.
21. **Bychkov, R., K. Pieper, C. Ried, M. Milosheva, E. Bychkov, F. C. Luft, and H. Haller.** 1999. Hydrogen peroxide, potassium currents, and membrane potential in human endothelial cells. Circulation **99:**1719–1725.
22. **Callapina, M., J. Zhou, T. Schmid, R. Kohl, and B. Brune.** 2005. NO restores HIF-1α hydroxylation during hypoxia: role of reactive oxygen species. Free Radic. Biol. Med. **39:**925–936.
23. **Canbolat, O., J. Fandrey, and W. Jelkmann.** 1998. Effects of modulators of the production and degradation of hydrogen peroxide on erythropoietin synthesis. Respir. Physiol. **114:**175–183.
24. **Cerutti, P. A.** 1985. Prooxidant states and tumor promotion. Science **227:**375–381.
25. **Chance, B., H. Sies, and A. Boveris.** 1979. Hydroperoxide metabolism in mammalian organs. Physiol. Rev. **59:**527–605.
26. **Chandel, N. S., D. S. McClintock, C. E. Feliciano, T. M. Wood, J. A. Melendez, A. M. Rodriguez, and P. T. Schumacker.** 2000. Reactive oxygen species generated at mitochondrial complex III stabilize hypoxia-inducible factor-1alpha during hypoxia: a mechanism of $O_2$ sensing. J. Biol. Chem. **275:**25130–25138.
27. **Chang, T. C., C. J. Huang, K. Tam, S. F. Chen, K. T. Tan, M. S. Tsai, T. N. Lin, and S. K. Shyue.** 2005. Stabilization of hypoxia-inducible factor-1α by prostacyclin under prolonged hypoxia via reducing reactive oxygen species level in endothelial cells. J. Biol. Chem. **280:**36567–36574.
28. **Chavez, J. C., F. Agani, P. Pichiule, and J. C. LaManna.** 2000. Expression of hypoxia-inducible factor-1α in the brain of rats during chronic hypoxia. J. Appl. Physiol. **89:**1937–1942.
29. **Chavez, J. C., and J. C. LaManna.** 2002. Activation of hypoxia-inducible factor-1 in the rat cerebral cortex after transient global ischemia: potential role of insulin-like growth factor-1. J. Neurosci. **22:**8922–8931.
30. **Chung-man Ho, J., S. Zheng, S. A. Comhair, C. Farver, and S. C. Erzurum.** 2001. Differential expression of manganese superoxide dismutase and catalase in lung cancer. Cancer Res. **61:**8578–8585.
31. **Deudero, J. J., C. Caramelo, M. C. Castellanos, F. Neria, R. Fernandez-Sanchez, O. Calabia, S. Penate, and F. R. Gonzalez-Pacheco.** 2008. Induction of hypoxia-inducible factor 1alpha gene expression by vascular endothelial growth factor. Role of a superoxide-mediated mechanism. J. Biol. Chem. **283:**11435–11444.
32. **Dirnagl, U., U. Lindauer, A. Them, S. Schreiber, H. W. Pfister, U. Koedel, R. Reszka, D. Freyer, and A. Villringer.** 1995. Global cerebral ischemia in the rat: online monitoring of oxygen free radical production using chemiluminescence in vivo. J. Cereb. Blood Flow Metab. **15:**929–940.
33. **Fandrey, J., S. Frede, and W. Jelkmann.** 1994. Role of hydrogen peroxide in hypoxia-induced erythropoietin production. Biochem. J. **303:**507–510.
34. **Gerald, D., E. Berra, Y. M. Frapart, D. A. Chan, A. J. Giaccia, D. Mansuy, J. Pouyssegur, M. Yaniv, and F. Mechta-Grigoriou.** 2004. JunD reduces tumor angiogenesis by protecting cells from oxidative stress. Cell **118:**781–794.
35. **Ginouves, A., K. Ilc, N. Macias, J. Pouyssegur, and E. Berra.** 2008. PHDs overactivation during chronic hypoxia "desensitizes" HIFα and protects cells from necrosis. Proc. Natl. Acad. Sci. USA **105:**4745–4750.
36. **Giorgio, M., M. Trinei, E. Migliaccio, and P. G. Pelicci.** 2007. Hydrogen peroxide: a metabolic by-product or a common mediator of ageing signals? Nat. Rev. Mol. Cell Biol. **8:**722–728.
37. **Gonzalez-Flecha, B., and B. Demple.** 1997. Homeostatic regulation of intracellular hydrogen peroxide concentration in aerobically growing *Escherichia coli*. J. Bacteriol. **179:**382–388.
38. **Gottlieb, E., and I. P. Tomlinson.** 2005. Mitochondrial tumour suppressors: a genetic and biochemical update. Nat. Rev. Cancer **5:**857–866.
39. **Grisham, M. B., L. A. Hernandez, and D. N. Granger.** 1986. Xanthine oxidase and neutrophil infiltration in intestinal ischemia. Am. J. Physiol. **251:**G567–G574.
40. **Guzy, R. D., B. Hoyos, E. Robin, H. Chen, L. Liu, K. D. Mansfield, M. C. Simon, U. Hammerling, and P. T. Schumacker.** 2005. Mitochondrial complex III is required for hypoxia-induced ROS production and cellular oxygen sensing. Cell. Metab. **1:**401–408.
41. **Guzy, R. D., and P. T. Schumacker.** 2006. Oxygen sensing by mitochondria

at complex III: the paradox of increased reactive oxygen species during hypoxia. Exp. Physiol. **91:**807–819.
42. **Guzy, R. D., B. Sharma, E. Bell, N. S. Chandel, and P. T. Schumacker.** 2008. Loss of the SdhB, but not the SdhA, subunit of complex II triggers reactive oxygen species-dependent hypoxia-inducible factor activation and tumorigenesis. Mol. Cell. Biol. **28:**718–731.
43. **Haddad, J. J., and S. C. Land.** 2001. A non-hypoxic, ROS-sensitive pathway mediates TNF-alpha-dependent regulation of HIF-1α. FEBS Lett. **505:** 269–274.
44. **Hagen, T., C. T. Taylor, F. Lam, and S. Moncada.** 2003. Redistribution of intracellular oxygen in hypoxia by nitric oxide: effect on HIF1α. Science **302:**1975–1978.
45. **Hederstedt, L.** 2003. Structural biology. Complex II is complex too. Science **299:**671–672.
46. **Herr, B., J. Zhou, S. Drose, and B. Brune.** 2007. The interaction of superoxide with nitric oxide destabilizes hypoxia-inducible factor-1α. Cell Mol. Life Sci. **64:**3295–3305.
47. **Holmquist, L., G. Stuchbury, M. Steele, and G. Munch.** 2007. Hydrogen peroxide is a true first messenger. J. Neural Transm. Suppl. **2007:**39–41.
48. **Ishii, N., M. Fujii, P. S. Hartman, M. Tsuda, K. Yasuda, N. Senoo-Matsuda, S. Yanase, D. Ayusawa, and K. Suzuki.** 1998. A mutation in succinate dehydrogenase cytochrome b causes oxidative stress and ageing in nematodes. Nature **394:**694–697.
49. **Ishii, T., K. Yasuda, A. Akatsuka, O. Hino, P. S. Hartman, and N. Ishii.** 2005. A mutation in the SDHC gene of complex II increases oxidative stress, resulting in apoptosis and tumorigenesis. Cancer Res. **65:**203–209.
50. **Jensen, R. L.** 2006. Hypoxia in the tumorigenesis of gliomas and as a potential target for therapeutic measures. Neurosurg. Focus **20:**E24.
51. **Jiang, Y., J. Wu, R. F. Keep, Y. Hua, J. T. Hoff, and G. Xi.** 2002. Hypoxia-inducible factor-1α accumulation in the brain after experimental intracerebral hemorrhage. J. Cereb. Blood Flow Metab. **22:**689–696.
52. **Jung, S. N., W. K. Yang, J. Kim, H. S. Kim, E. J. Kim, H. Yun, H. Park, S. S. Kim, W. Choe, I. Kang, and J. Ha.** 2008. Reactive oxygen species stabilize hypoxia inducible factor-1 alpha protein and stimulate transcriptional activity via AMP-activated protein kinase in DU145 human prostate cancer cells. Carcinogenesis **29:**713–721.
53. **King, A., M. A. Selak, and E. Gottlieb.** 2006. Succinate dehydrogenase and fumarate hydratase: linking mitochondrial dysfunction and cancer. Oncogene **25:**4675–4682.
54. **Kohl, R., J. Zhou, and B. Brune.** 2006. Reactive oxygen species attenuate nitric-oxide-mediated hypoxia-inducible factor-1α stabilization. Free Radic. Biol. Med. **40:**1430–1442.
55. **Koivunen, P., M. Hirsila, A. M. Remes, I. E. Hassinen, K. I. Kivirikko, and J. Myllyharju.** 2007. Inhibition of hypoxia-inducible factor (HIF) hydroxylases by citric acid cycle intermediates: possible links between cell metabolism and stabilization of HIF. J. Biol. Chem. **282:**4524–4532.
56. **Kozhukhar, A. V., I. M. Yasinska, and V. V. Sumbayev.** 2006. Nitric oxide inhibits HIF-1α protein accumulation under hypoxic conditions: implication of 2-oxoglutarate and iron. Biochimie **88:**411–418.
57. **Kwon, S. J., J. J. Song, and Y. J. Lee.** 2005. Signal pathway of hypoxia-inducible factor-1α phosphorylation and its interaction with von Hippel-Lindau tumor suppressor protein during ischemia in MiaPaCa-2 pancreatic cancer cells. Clin. Cancer Res. **11:**7607–7613.
58. **Lacy, F., M. T. Kailasam, D. T. O'Connor, G. W. Schmid-Schonbein, and R. J. Parmer.** 2000. Plasma hydrogen peroxide production in human essential hypertension: role of heredity, gender, and ethnicity. Hypertension **36:**878–884.
59. **Laurent, A., C. Nicco, C. Chereau, C. Goulvestre, J. Alexandre, A. Alves, E. Levy, F. Goldwasser, Y. Panis, O. Soubrane, B. Weill, and F. Batteux.** 2005. Controlling tumor growth by modulating endogenous production of reactive oxygen species. Cancer Res. **65:**948–956.
60. **Leonardi, F., L. Attorri, R. D. Benedetto, A. D. Biase, M. Sanchez, F. P. Tregno, M. Nardini, and S. Salvati.** 2007. Docosahexaenoic acid supplementation induces dose and time dependent oxidative changes in C6 glioma cells. Free Radic. Res. **41:**748–756.
61. **Lopez-Lazaro, M.** 2007. Dual role of hydrogen peroxide in cancer: possible relevance to cancer chemoprevention and therapy. Cancer Lett. **252:**1–8.
62. **Lovstad, R. A.** 2003. A kinetic study on iron stimulation of the xanthine oxidase dependent oxidation of ascorbate. Biometals **16:**435–439.
63. **Lu, H., C. L. Dalgard, A. Mohyeldin, T. McFate, A. S. Tait, and A. Verma.** 2005. Reversible inactivation of HIF-1 prolyl hydroxylases allows cell metabolism to control basal HIF-1. J. Biol. Chem. **280:**41928–41939.
64. **MacKenzie, E. D., M. A. Selak, D. A. Tennant, L. J. Payne, S. Crosby, C. M. Frederiksen, D. G. Watson, and E. Gottlieb.** 2007. Cell-permeating alpha-ketoglutarate derivatives alleviate pseudohypoxia in succinate dehydrogenase-deficient cells. Mol. Cell. Biol. **27:**3282–3289.
65. **Makino, N., K. Sasaki, K. Hashida, and Y. Sakakura.** 2004. A metabolic model describing the $H_2O_2$ elimination by mammalian cells including $H_2O_2$ permeation through cytoplasmic and peroxisomal membranes: comparison with experimental data. Biochim. Biophys. Acta **1673:**149–159.
66. **Mansfield, K. D., R. D. Guzy, Y. Pan, R. M. Young, T. P. Cash, P. T. Schumacker, and M. C. Simon.** 2005. Mitochondrial dysfunction resulting from loss of cytochrome c impairs cellular oxygen sensing and hypoxic HIF-alpha activation. Cell. Metab. **1:**393–399.
67. **Meng, Q., Y. T. Wong, J. Chen, and R. Ruan.** 2007. Age-related changes in mitochondrial function and antioxidative enzyme activity in Fischer 344 rats. Mech. Ageing Dev. **128:**286–292.
68. **Moeller, B. J., Y. Cao, C. Y. Li, and M. W. Dewhirst.** 2004. Radiation activates HIF-1 to regulate vascular radiosensitivity in tumors: role of reoxygenation, free radicals, and stress granules. Cancer Cell **5:**429–441.
69. **Nakamura, J., E. R. Purvis, and J. A. Swenberg.** 2003. Micromolar concentrations of hydrogen peroxide induce oxidative DNA lesions more efficiently than millimolar concentrations in mammalian cells. Nucleic Acids Res. **31:**1790–1795.
70. **Page, E. L., D. A. Chan, A. J. Giaccia, M. Levine, and D. E. Richard.** 2008. Hypoxia-inducible factor-1α stabilization in nonhypoxic conditions: role of oxidation and intracellular ascorbate depletion. Mol. Biol. Cell **19:**86–94.
71. **Pan, Y., K. D. Mansfield, C. C. Bertozzi, V. Rudenko, D. A. Chan, A. J. Giaccia, and M. C. Simon.** 2007. Multiple factors affecting cellular redox status and energy metabolism modulate hypoxia-inducible factor prolyl hydroxylase activity in vivo and in vitro. Mol. Cell. Biol. **27:**912–925.
72. **Park, S., X. You, and J. A. Imlay.** 2005. Substantial DNA damage from submicromolar intracellular hydrogen peroxide detected in Hpx- mutants of Escherichia coli. Proc. Natl. Acad. Sci. USA **102:**9317–9322.
73. **Peters, O., T. Back, U. Lindauer, C. Busch, D. Megow, J. Dreier, and U. Dirnagl.** 1998. Increased formation of reactive oxygen species after permanent and reversible middle cerebral artery occlusion in the rat. J. Cereb. Blood Flow Metab. **18:**196–205.
74. **Pollard, P. J., J. J. Briere, N. A. Alam, J. Barwell, E. Barclay, N. C. Wortham, T. Hunt, M. Mitchell, S. Olpin, S. J. Moat, I. P. Hargreaves, S. J. Heales, Y. L. Chung, J. R. Griffiths, A. Dalgleish, J. A. McGrath, M. J. Gleeson, S. V. Hodgson, R. Poulsom, P. Rustin, and I. P. Tomlinson.** 2005. Accumulation of Krebs cycle intermediates and over-expression of HIF1α in tumours which result from germline FH and SDH mutations. Hum. Mol. Genet. **14:**2231–2239.
75. **Pouyssegur, J., and F. Mechta-Grigoriou.** 2006. Redox regulation of the hypoxia-inducible factor. Biol. Chem. **387:**1337–1346.
76. **Powell, F. L.** 2003. Functional genomics and the comparative physiology of hypoxia. Annu. Rev. Physiol. **65:**203–230.
77. **Qutub, A. A., and A. S. Popel.** 2006. A computational model of intracellular oxygen sensing by hypoxia-inducible factor HIF1 alpha. J. Cell Sci. **119:** 3467–3480.
78. **Qutub, A. A., and A. S. Popel.** 2007. Three autocrine feedback loops determine HIF1 alpha expression in chronic hypoxia. Biochim. Biophys. Acta **1773:**1511–1525.
79. **Schlegel, H. G.** 1977. Aeration without air: oxygen supply by hydrogen peroxide. Biotechnol. Bioeng. **19:**413–424.
80. **Schraufstatter, I., P. A. Hyslop, J. H. Jackson, and C. G. Cochrane.** 1988. Oxidant-induced DNA damage of target cells. J. Clin. Investig. **82:**1040–1050.
81. **Schroedl, C., D. S. McClintock, G. R. Budinger, and N. S. Chandel.** 2002. Hypoxic but not anoxic stabilization of HIF-1alpha requires mitochondrial reactive oxygen species. Am. J. Physiol. Lung Cell Mol. Physiol. **283:**L922–L931.
82. **Seaver, L. C., and J. A. Imlay.** 2001. Hydrogen peroxide fluxes and compartmentalization inside growing *Escherichia coli*. J. Bacteriol. **183:**7182–7189.
83. **Selak, M. A., S. M. Armour, E. D. MacKenzie, H. Boulahbel, D. G. Watson, K. D. Mansfield, Y. Pan, M. C. Simon, C. B. Thompson, and E. Gottlieb.** 2005. Succinate links TCA cycle dysfunction to oncogenesis by inhibiting HIF-alpha prolyl hydroxylase. Cancer Cell **7:**77–85.
84. **Selak, M. A., R. V. Duran, and E. Gottlieb.** 2006. Redox stress is not essential for the pseudo-hypoxic phenotype of succinate dehydrogenase deficient cells. Biochim. Biophys. Acta **1757:**567–572.
85. **Semenza, G. L.** 2004. Hydroxylation of HIF-1: oxygen sensing at the molecular level. Physiology (Bethesda) **19:**176–182.
86. **Senoo-Matsuda, N., K. Yasuda, M. Tsuda, T. Ohkubo, S. Yoshimura, H. Nakazawa, P. S. Hartman, and N. Ishii.** 2001. A defect in the cytochrome b large subunit in complex II causes both superoxide anion overproduction and abnormal energy metabolism in Caenorhabditis elegans. J. Biol. Chem. **276:**41553–41558.
87. **Srinivas, V., I. Leshchinsky, N. Sang, M. P. King, A. Minchenko, and J. Caro.** 2001. Oxygen sensing and HIF-1 activation does not require an active mitochondrial respiratory chain electron-transfer pathway. J. Biol. Chem. **276:**21995–21998.
88. **Stone, J. R., and S. Yang.** 2006. Hydrogen peroxide: a signaling messenger. Antioxid. Redox Signal. **8:**243–270.
89. **Sumbayev, V. V., and I. M. Yasinska.** 2006. Peroxynitrite as an alternative donor of oxygen in HIF-1α proline hydroxylation under low oxygen availability. Free Radic. Res. **40:**631–635.
90. **Szatrowski, T. P., and C. F. Nathan.** 1991. Production of large amounts of hydrogen peroxide by human tumor cells. Cancer Res. **51:**794–798.
91. **Szeto, S. S., S. N. Reinke, B. D. Sykes, and B. D. Lemire.** 2007. Ubiquinone-binding site mutations in the Saccharomyces cerevisiae succinate dehydro-

genase generate superoxide and lead to the accumulation of succinate. J. Biol. Chem. **282:**27518–27526.

92. **Tanriverdi, T., H. Hanimoglu, T. Kacira, G. Z. Sanus, R. Kemerdere, P. Atukeren, K. Gumustas, B. Canbaz, and M. Y. Kaynar.** 2007. Glutathione peroxidase, glutathione reductase and protein oxidation in patients with glioblastoma multiforme and transitional meningioma. J. Cancer Res. Clin. Oncol. **133:**627–633.
93. **Teixeira, H. D., R. I. Schumacher, and R. Meneghini.** 1998. Lower intracellular hydrogen peroxide levels in cells overexpressing CuZn-superoxide dismutase. Proc. Natl. Acad. Sci. USA **95:**7872–7875.
94. **Tuttle, S. W., A. Maity, P. R. Oprysko, A. V. Kachur, I. S. Ayene, J. E. Biaglow, and C. J. Koch.** 2007. Detection of reactive oxygen species via endogenous oxidative pentose phosphate cycle activity in response to oxygen concentration: implications for the mechanism of HIF-1α stabilization under moderate hypoxia. J. Biol. Chem. **282:**36790–36796.
95. **Vangeison, G., D. Carr, H. J. Federoff, and D. A. Rempe.** 2008. The good, the bad, and the cell type-specific roles of hypoxia inducible factor-1 alpha in neurons and astrocytes. J. Neurosci. **28:**1988–1993.
96. **Vaux, E. C., E. Metzen, K. M. Yeates, and P. J. Ratcliffe.** 2001. Regulation of hypoxia-inducible factor is preserved in the absence of a functioning mitochondrial respiratory chain. Blood **98:**296–302.
97. **Vordermark, D., and J. M. Brown.** 2003. Evaluation of hypoxia-inducible factor-1α (HIF-1α) as an intrinsic marker of tumor hypoxia in U87 MG human glioblastoma: in vitro and xenograft studies. Int. J. Radiat. Oncol. Biol. Phys. **56:**1184–1193.
98. **Wang, G. L., B. H. Jiang, E. A. Rue, and G. L. Semenza.** 1995. Hypoxia-inducible factor 1 is a basic-helix-loop-helix-PAS heterodimer regulated by cellular $O_2$ tension. Proc. Natl. Acad. Sci. USA **92:**5510–5514.
99. **Wartenberg, M., F. C. Ling, M. Muschen, F. Klein, H. Acker, M. Gassmann, K. Petrat, V. Putz, J. Hescheler, and H. Sauer.** 2003. Regulation of the multidrug resistance transporter P-glycoprotein in multicellular tumor spheroids by hypoxia-inducible factor (HIF-1) and reactive oxygen species. FASEB J. **17:**503–505.
100. **Wellman, T. L., J. Jenkins, P. L. Penar, B. Tranmer, R. Zahr, and K. M. Lounsbury.** 2004. Nitric oxide and reactive oxygen species exert opposing effects on the stability of hypoxia-inducible factor-1α (HIF-1α) in explants of human pial arteries. FASEB J. **18:**379–381.
101. **Williams, N., and J. Yandell.** 1982. Outer-sphere electron transfer of ascorbate anions. Aust. J. Chem. **35:**1133–1144.
102. **Xia, C., Q. Meng, L. Z. Liu, Y. Rojanasakul, X. R. Wang, and B. H. Jiang.** 2007. Reactive oxygen species regulate angiogenesis and tumor growth through vascular endothelial growth factor. Cancer Res. **67:** 10823–10830.
103. **Yang, Z. Z., A. Y. Zhang, F. X. Yi, P. L. Li, and A. P. Zou.** 2003. Redox regulation of HIF-1alpha levels and HO-1 expression in renal medullary interstitial cells. Am. J. Physiol. Renal Physiol. **284:**F1207–F1215.
104. **Yankovskaya, V., R. Horsefield, S. Tornroth, C. Luna-Chavez, H. Miyoshi, C. Leger, B. Byrne, G. Cecchini, and S. Iwata.** 2003. Architecture of succinate dehydrogenase and reactive oxygen species generation. Science **299:** 700–704.
105. **Zhong, W., T. Yan, R. Lim, and L. W. Oberley.** 1999. Expression of superoxide dismutases, catalase, and glutathione peroxidase in glioma cells. Free Radic. Biol. Med. **27:**1334–1345.